The Theory and Practical Application of Antitriptic Balance

J. T. Schaefer and C. A. Doswell III

Techniques Development Unit, National Severe Storms Forecast Center, Kansas City, MO

ABSTRACT

A flow where the pressure gradient, Coriolis and viscous forces are balanced is examined. It is found that such a flow is a reasonable approximation to the "steady state" flow in the vicinity of the contact layer. Kinematic effects implicit in the adjustment of an arbitrary flow to this balanced state are examined and can be used to explain several features of the nocturnal low-level jet. A method to use this balanced flow operationally to infer Ekman layer features is developed and several cases are examined.

1. Introduction

A well-known dichotomy exists in the density of meteorological observations. That is, surface observations are taken hourly over a network with an average spacing of ~100 km, while upper air data are collected at 12 h intervals from points separated by ~400 km. A major problem with this arrangement is that dense quantitative data are only available in the frictionally dominated surface-contact layer. However, convective processes are highly dependent on the kinematic and thermodynamic properties of the atmosphere above the surface layer, but below the cloud layer itself. Because of frictional effects, kinematic fields computed from surface data do not necessarily reflect significant subcloud-layer processes (e.g., Day, 1953). While there is some agreement between surface convergence and convective clouds (Ulanski and Garstang, 1978), the convergence pattern may undergo rapid changes across the lowest tens of millibars (Ogura and Chen, 1977). Thus, to diagnose impending severe convection, techniques which allow the forecaster to infer processes occurring above the lowest atmospheric layer from surface data alone need to be developed.

In order to do this, it is convenient to subdivide the atmospheric boundary layer. To a first approximation the lowest sublayer (of order 100 m deep), the contact layer, can be considered as a layer of constant stress (Tennekes and Lumley, 1972, p. 169). Within this layer, wind direction is effectively constant with height while wind speed varies as a function of the local roughness, heat flux and momentum flux. Above the contact layer is the so-called Ekman layer. Here an approximate balance among pressure, Coriolis and the height-varying frictional forces exists. This is a region of transition between the friction layer and the quasi-geostrophic free atmosphere and extends to heights of order 1 km.

At levels well into the Ekman layer, the variation of frictional stress with height makes surface data inadequate for the determination of flow characteristics. However, as a direct result of the effectively constant stress near the earth's surface, reliable inferences about the flow field immediately above the contact layer can be made exclusively from surface data.

2. Antitriptic flow

A primary motivation for trying to develop a means for estimating the flow at the top of the contact layer is that geostrophic equilibrium is inherently inappropriate as an approximation to the steady-state flow there. This is manifest when considering ageostrophic accelerations implied from surface data. Doswell (1976) shows that surface geostrophic flow is typically so far in excess of the observed winds that the ageostrophic vorticity is essentially identical to the geostrophic vorticity with a change in sign. Thus, geostrophic equilibrium concepts (e.g., Saucier, 1955, p. 240ff) cannot be used effectively to resolve contact-layer accelerations.

We define antitriptic flow as one characterized by an equilibrium among Coriolis, pressure and frictional forces (Saucier, 1955, p. 242).[1] Since only surface data are available, friction is parameterized by assuming that the stress is directed opposite to the wind, and with magnitude proportional to the wind speed (Guldburg and Mohn, 1876).

---

[1] Note that this definition differs from that in the *Glossary of Meteorology* (Huschke, 1959) which excludes Coriolis force.

Antitriptic balance is then expressed as

$$-f\hat{\mathbf{k}} \times \mathbf{v}_a - \alpha\nabla p - K\mathbf{v}_a = 0, \qquad (1)$$

where

f Coriolis parameter
$\mathbf{v}_a$ antitriptic wind
α specific volume
∇p horizontal pressure ascendent
K Guldburg-Mohn coefficient
$\hat{\mathbf{k}}$ unit vector pointing vertically.

If the pressure gradient force is replaced by the geostrophic wind, (1) can be solved for the antitriptic wind, i.e.,

$$\mathbf{v}_a = \frac{1}{(1 + \beta^2)} (\mathbf{v}_g - \beta\mathbf{v}_g \times \hat{\mathbf{k}}), \qquad (2)$$

where

$$\mathbf{v}_g = \hat{\mathbf{k}} \times \frac{\alpha}{f} \nabla p, \quad \beta = K/f.$$

Eq. (2) defines a circle of diameter $|\mathbf{v}_g|$ centered at the midpoint of the geostrophic wind vector. Note that the backing angle between the antitriptic and geostrophic directions is the inverse tangent of β (Fig. 1). As indicated by Arya (1978), the isobaric crossing angle is directly proportional to the magnitude of the viscous force (K) and inversely proportional to the Coriolis parameter (f). When β vanishes $(K = 0)$, the antitriptic wind equals the geostrophic wind. A 45° turn to the left of the actual wind relative to the geostrophic wind (expected at the bottom of the Ekman spiral) occurs when $\beta = 1$ $(K = f)$. As β approaches positive infinity $(K \to +\infty$ or $f \to 0)$, the antitriptic wind approaches zero. Mathematically, antitriptic flow can be directed to the right of the geostrophic flow only if the Guldburg-Mohn coefficient is negative. However, this is physically impossible since the closure assumption requiring friction to retard the flow is violated.

If the antitriptic wind, rather than the geostrophic, is used to replace the pressure gradient force in the equation of motion, accelerations can be expressed in terms of antitriptic deviations, i.e.,

$$\frac{D}{Dt} \mathbf{v} = -f\hat{\mathbf{k}} \times (\mathbf{v} - \mathbf{v}_a) - K(\mathbf{v} - \mathbf{v}_a), \qquad (3)$$

where $D/Dt \equiv \partial/\partial t + \mathbf{v}\cdot\nabla + w(\partial/\partial z)$ is the substantial derivative and $\mathbf{v}$ is the actual wind. For illustration, we consider horizontal flow with small Rossby number, so that the substantial derivative can be replaced by the partial derivative with respect to time. By using complex notation $(V = u + iv$, etc.), Eq. (3) can be rewritten as

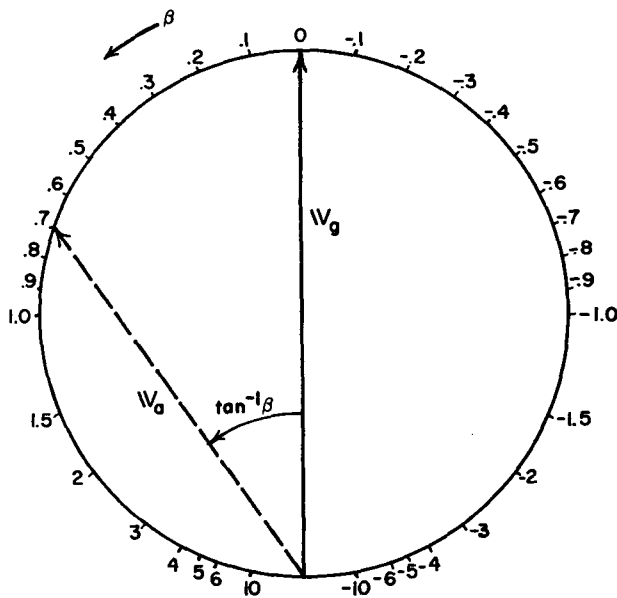$$\frac{\partial V}{\partial t} + ifV = -KV + (if + K)V_a. \qquad (4)$$

FIG. 1. Relationship between geostrophic and antitriptic winds (example is for $\beta = 0.7$).

Since (4) is a first-order differential equation, the time-varying part of the solution can be written immediately as

$$V = (V_0 - V_a)e^{-(if+K)t} + V_a, \qquad (5)$$

where V_0 is the initial wind vector. The solution, Eq. (5), is the equation of a logarithmic spiral. That is, the antitriptic deviation follows a damped inertial circle, with the damping having an e-folding time of K^{-1} (Fig. 2). For a K of 5×10^{-5} s^{-1}, this time is about 5.5 h.

The existence of such a transient solution is well known (e.g., Starr, 1945). Across the Ekman layer, the e-folding time increases rapidly with height (Ching and Businger, 1968), so that at points well above the contact layer, periodic modes dominate motion and approximate inertial solutions are obtained (Bonner and Paegle, 1970). However, near the top of the contact layer, the rapid damping of the transient makes the antitriptic concept a reasonable approximation to the steady-state flow.

3. Kinematic analysis

While closure via a Guldburg-Mohn coefficient fails to consider such things as shear and buoyancy effects explicitly, its simplicity allows an elucidation of basic physical principles which can be masked by more elegant techniques (e.g., Mellor and Yamada, 1974). For example, Defant (1951) has used an equation of motion similar to (3) to explain many of the significant features of the sea breeze. Also, interactions between the boundary layer and the free atmosphere have been examined by Mahrt
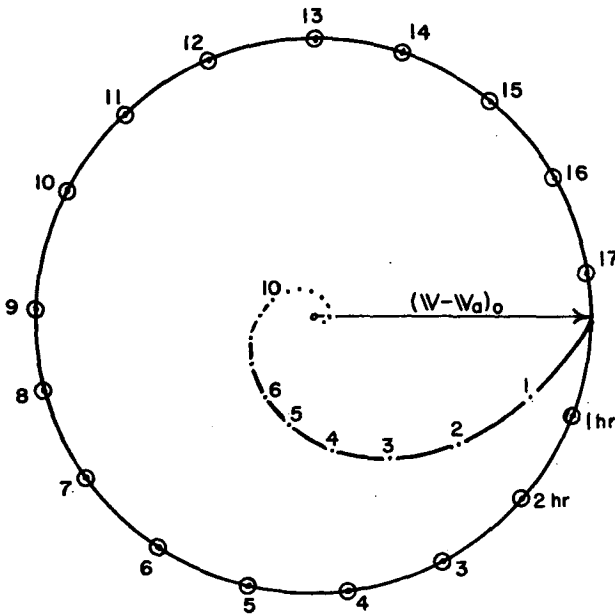
FIG. 2. Temporal behavior of antitriptic adjustment at 1 h intervals. The outer circle represents a pure inertial oscillation.

and Park (1976) using a modification of the Guldburg-Mohn closure.

Here we wish to examine the implications of antitriptic flow on the kinematic structure near the top of the contact layer. Straightforward scale considerations can be used to show that antitriptic divergence (D_a), which is an estimate of steady-state divergence in the Ekman layer, is approximated by

$$D_a = \frac{-\beta}{(1 + \beta^2)} \xi_g. \qquad (6)$$

Simply stated, equilibrium boundary-layer divergence has a direct negative correlation with geostrophic vorticity. This result is well-known from Ekman theory and is generally referred to as "Ekman pumping." Similarly, the antitriptic vertical component of vorticity (ξ_a) is approximated by

$$\xi_a = \frac{1}{(1 + \beta^2)} \xi_g. \qquad (7)$$

Remembering that $\beta \equiv K/f$, several conclusions can be immediately drawn from (6) and (7). As the friction coefficient increases, the antitriptic vorticity decreases. However, the effect of frictional damping on divergence is not monotonic. Increasing the frictional dissipation increases the magnitude of divergence only for turning angles $< 45°$ (at 45°, the Guldberg-Mohn coefficient equals the Coriolis parameter). For larger turning angles, increasing frictional effects decrease the magnitude of the anti-

triptic divergence. That is, at high turning angles, frictional retardation dominates the shunting of the flow toward lower pressure, and viscous effects damp low-level vertical velocities. This effect is independent of the strength of the pressure system. Such a relationship between divergence and the amount of viscous damping has also been noted by Mahrt (1975) and Paegle and Paegle (1978). Decreasing the latitude has the same effect as increasing the frictional coefficient.

If terms involving the derivatives of f and K are ignored via scale considerations, small Rossby number approximations to the divergence and vorticity tendencies are found from (3) to be

$$\frac{\partial D}{\partial t} = f(\xi - \xi_a) - K(D - D_a), \qquad (8)$$

$$\frac{\partial \xi}{\partial t} = -f(D - D_a) - K(\xi - \xi_a). \qquad (9)$$

The system (8) and (9) can be solved analytically. Under constant antitriptic forcing, the divergence and vorticity develop from an initial state (D_0, ξ_0) according to

$$D(t) = [(D_0 - D_a) \cos ft$$
$$+ (\xi_0 - \xi_a) \sin ft] e^{-Kt} + D_a, \qquad (10)$$

$$\xi(t) = [(\xi_0 - \xi_a) \cos ft$$
$$- (D_0 - D_a) \sin ft] e^{-Kt} + \xi_a. \qquad (11)$$

The time-varying part of the solution for the complex variable $(D + i\xi)$ describes a logarithmic spiral.

To examine this solution, we assume that the ratio between the initial divergence and vorticity is maintained under antitriptic balance, i.e.,

$$\frac{\xi_0}{D_0} = \frac{\xi_a}{D_a}. \qquad (12)$$

Although this initial state is certainly an arbitrary one, it allows the examination of the solution's behavior, without requiring the consideration of a wide range of similarly arbitrary specifications for (ξ_0, D_0). From (6) and (7) this ratio, to the same order of approximation, is simply $-f/K$. After trigonometric manipulation, Eqs. (10) and (11) can be written as

$$\frac{D}{D_a} = \frac{(D_0 - D_a)}{D_a} \left[\left(1 - \frac{f}{K} \right) \sin ft \right.$$
$$+ \left. \sqrt{2} \cos \left(\frac{\pi}{4} + ft \right) \right] e^{-Kt} + 1$$
$$\equiv \frac{(D_0 - D_a)}{D_a} \Psi(t) + 1, \qquad (13)$$

$$\frac{\xi}{\xi_a} = \frac{(D_0 - D_a)}{D_a}\left[\left(\frac{K}{f} - 1\right)\sin ft\right.$$

$$\left. + \sqrt{2}\cos\left(ft - \frac{\pi}{4}\right)\right]e^{-Kt} + 1$$

$$\equiv -\frac{(D_0 - D_a)}{D_a}\Phi(t) + 1, \quad (14)$$

where $\Psi(t)$ and $\Phi(t)$ represent the time-varying parts of the divergence and vorticity, respectively.

During antitriptic adjustment, both the divergence and vorticity undergo a damped oscillation about antitriptic equilibrium. However, for turning angles $> 17.7°$ ($K/f > 1/\pi$), the half-period of the oscillations (π/f) is greater than the e-folding time. Thus, most of the adjustment has taken place after only one-half of an oscillation. Further, for antitriptic turning angles $< 67.5°$, the major portion of the divergence oscillation (the cosine terms) is 90° out of phase with that of the vorticity (Fig. 3). This phase shift causes the first minimum of the divergence transient to be larger than that of the vorticity transient by a factor R, where

$$R = \frac{f}{K}\exp[(\pi/2)(f/K)]. \quad (15)$$

This ratio has an absolute minimum value of 4.27 when the turning angle is 36° ($K/f = \pi/2$). Therefore, generally speaking, while the vorticity adjusts to its antitriptic value in a nearly monotonic manner, the divergence can overshoot its equilibrium (antitriptic) state by a significant amount.

4. The low-level jet

Several of the effects predicted by antitriptic theory can be observed in association with the low-level jet of the Great Plains. The diurnal variation of frictional damping across the boundary layer is one of the causes of this phenomenon. This jet stream shows a diurnal variation in wind velocities with maximum speeds occurring between 0000 and 0300 LST. Nocturnal thunderstorms, which are frequent over the Great Plains, are highly correlated with this synoptic disturbance.

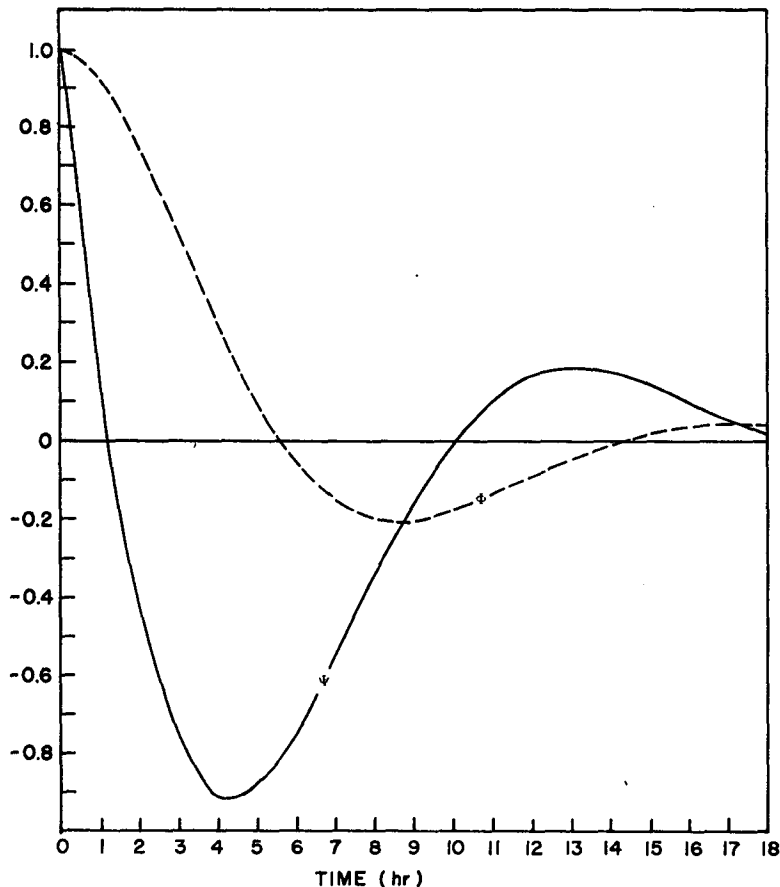Bonner and Paegle (1970) have shown that the wind near the top of the contact layer rotates

FIG. 3. Temporal variation of divergence (Ψ) and vorticity (Φ) during adjustment for $\beta = 0.5$ (30° turning angle).
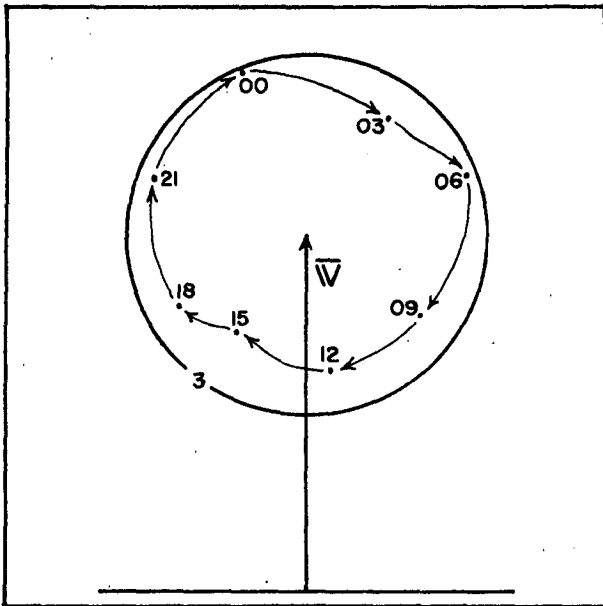
FIG. 4. Hodograph of mean wind variation at 320 m above the ground, at Ft. Worth, Texas, July and August 1958–64; times are CST (after Bonner and Paegle, 1970).

around its temporal mean vector in a clockwise sense at a rate which is fastest in the evening and slows toward dawn (Fig. 4). The nocturnal hours of this cycle are similar to the first portion of the antitriptic adjustment spiral (Fig. 2). As the depth of the contact layer decreases in the early evening, the wind above is forced out of antitriptic balance by

the decreased importance of friction. However, viscosity remains finite and is a factor in the subsequent adjustment.

The low-level winds do not describe an inertial circle but rather are driven toward antitriptic balance. If the low-level jet is primarily a rotating ageostrophic wind in a constant geostrophic wind field, by 0600 CST the observed winds should be directed to the right of the geostrophic vector (toward higher pressure). A study of the mean kinematic features of 10 low-level jet cases at 0600 CST (Bonner et al., 1968) found that the actual wind is always directed to the left of the geostrophic wind. This is consistent with the rapidly damped circle required by antitriptic theory.

Further, the marked temporal changes in the vertical velocity field associated with the low-level jet indicate that a mechanism other than Ekman pumping is operating. Bonner (1966) presents two vertical velocity fields separated by 12 h in a jet-relative coordinate system. The patterns are quite complicated (Fig. 5). At 1800 CST the right rear quadrant of the jet is a region of descent, with maximum ascent upstream and to the left of the velocity core. By 0600 CST the next morning, the subsidence has virtually disappeared, with almost all of the jet region showing ascending motions. Also, the region of maximum ascent has moved to a position *along* the jet axis.

Although these changes are complex, the simplified divergence tendency can provide some explanation. While undergoing antitriptic adjustment, the
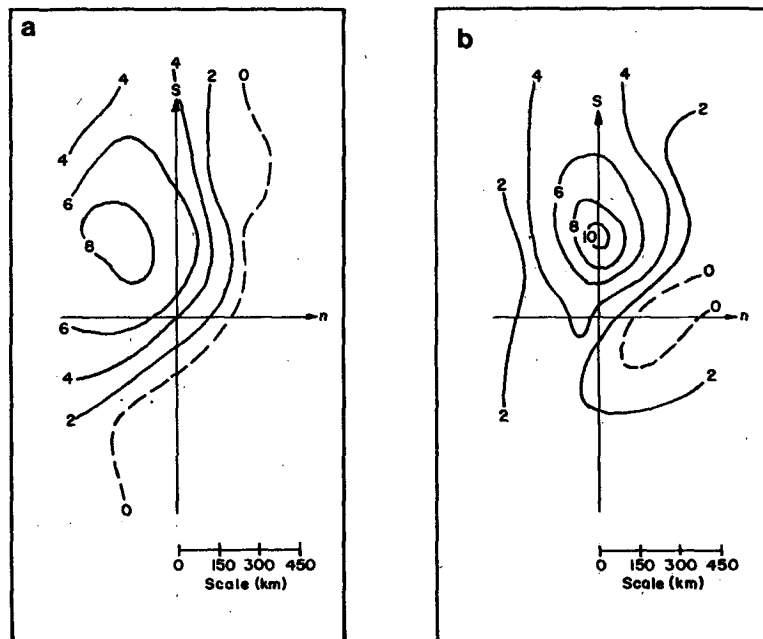

FIG. 5. Vertical velocities at 2500 m in jet coordinate system (after Bonner, 1966):
(a) 1800 CST 16 May, 1961; (b) 0600 CST 17 May 1961.

divergence (and thus the vertical velocity) undergoes a damped oscillation. Regions characterized by large departures from antitriptic balance (e.g., near the low-level jet stream core) are expected to show the largest oscillations during the adjustment process. Fig. 5 reveals this to be the case. Obviously, the simple theory presented here cannot reasonably be expected to be quantitatively tested against real data. Relating the vertical velocity field to the antitriptic divergence field requires several approximations which are not strictly valid: specifically, 1) the geostrophic wind is not constant but, rather, has a large diurnal variation; 2) the nonlinear terms are not negligible in the case of a low-level jet; 3) the turning angle is not typically constant in space and time; 4) there is no *a priori* reason to believe that (12) is a valid assumption; and 5) frictional stress depends on more factors than just the vector wind at the surface. Thus, a quantitative test is not expected to be very revealing. The low-level jet is more complicated than this simple theory implies. However, these results suggest that the temporal variation of the divergence field may be, at least partially, a response to the antitriptic adjustment process.

5. An operational antitriptic closure

Practical application of the antitriptic concept requires a method of determining the Guldburg-Mohn coefficient exclusively from surface data. Conceptually, this problem is similar to the search for a surface-data-determined drag coefficient. Cressman (1960) approximates the drag coefficient simply as a function of the mean topography. Lewis (1971) uses the Cressman drag coefficient to specify the Guldburg-Mohn parameter. By applying variational techniques, he develops an analysis that is constrained by antitriptic adjustment.

However, Wilkins and Sasaki (1970) have demonstrated that the drag coefficient is not prescribed solely by surface roughness. Rather, drag is proportional to the ratio of the integrated boundary layer convergence to the boundary layer vorticity. Their formulation is equivalent to solving (6) and (7) for K, i.e.,

$$K = -f \frac{D_a}{\xi_a} .$$ (16)

The problem with this specification is that (16) requires an estimate of the antitriptic divergence and vorticity before the Guldburg-Mohn coefficient can be computed. However, computation of D_a and ξ_a requires that K be known.

This paradoxical situation can be resolved by noting that (2) requires the angle ϕ between the antitriptic wind and the geostrophic wind to be

$$\tan\phi = \frac{\mathbf{v}_a \times \mathbf{v}_g \cdot \hat{\mathbf{k}}}{\mathbf{v}_a \cdot \mathbf{v}_g} = \beta.$$ (17)

Further, surface frictional stress is approximately directed along the anemometer winds. By definition, the frictional stress also parallels the antitriptic winds. For observed winds denoted by $\mathbf{v}_0$, this requires

$$\mathbf{v}_0 = \frac{|\mathbf{v}_0|}{|\mathbf{v}_a|} \mathbf{v}_a.$$ (18)

Therefore, the Guldburg-Mohn coefficient can be estimated by computing the geostrophic turning angle of the observed surface winds, using (18) in (17).

Geostrophic winds are computed via the Bellamy altimeter correction method (Bonner and Paegle, 1970), to account for diurnal effects over the sloping terrain. Since the geostrophic wind is computed at grid points while the actual wind is observed at quasi-random sites, direct application of (17) is not possible. Not only is vector interpolation to grid points a non-unique process (Schaefer and Doswell, 1979), but local topographic effects can often bias individual wind observations. Thus, in evaluating K, a local average value of the turning angle must be used, as suggested by Wilkins and Sasaki (1970).

The local averaging is done via a simple arithmetic mean of the turning angles at the data points within a square, six grid spaces on a side, centered at the grid point in question. While this process is somewhat arbitrary, it has the desired result of eliminating negative K values. Objective interpolation for operational application is accomplished with a single-pass Gaussian weight function (Doswell, 1977), with data exterior to the grid (out to two grid spaces) included in the interpolation.

6. Operational use of antitriptic balance

One use commonly made of surface data for severe weather forecasting is the computation of moisture flux convergence. Hudson (1971) has found that well-defined areas of moisture convergence are typically associated with intense convection, while Negri *et al.* (1977) demonstrate the need for moisture flux convergence, especially when well-defined synoptic-scale disturbances are not present. Because surface flow is not always representative of the storm inflow region—i.e., the "roots" of the convection are not always in the contact layer—it is suggested that the antitriptic wind $\mathbf{v}_a$ should be a better indicator of impending storm development than the surface wind. Accordingly, for operational applications the gridded values of $\mathbf{v}_a$ are used to compute antitriptic moisture flux convergence

$$\nabla \cdot (r\mathbf{v}_a) = m^2 \left[\frac{\partial}{\partial x} \left(\frac{ru_a}{m} \right) + \frac{\partial}{\partial y} \left(\frac{rv_a}{m} \right) \right] ,$$ (19)
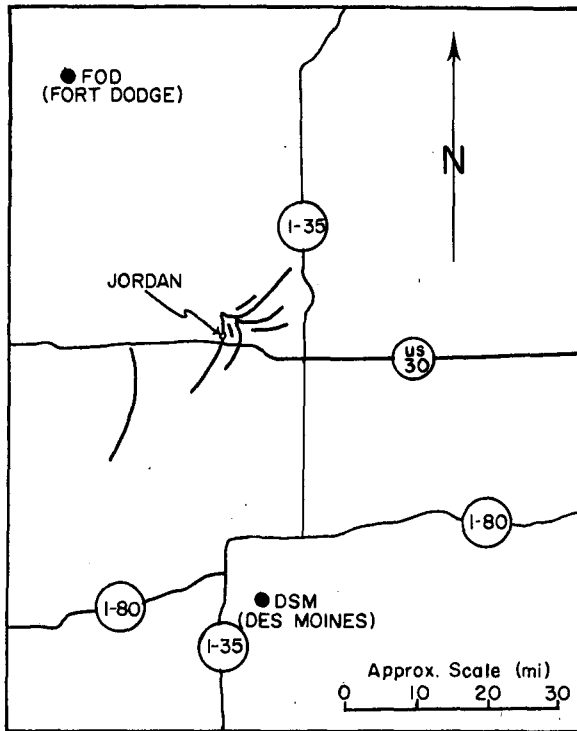
FIG. 6. Tornado tracks on 13 June 1976 in central Iowa
(after Brown and Knupp, 1980).

where m is the metric coefficient for the map projection and r is the mixing ratio near the top of the contact layer where antitriptic balance is apropos.

While the value of mixing ratio at this level is not known, Schaefer (1976) has found that during the afternoon hours the mixing ratio above the contact layer is $(80 \pm 10\%)$ of the surface value. Thus, within the accuracy of the antitriptic assumption itself, the surface mixing ratio can be considered as representative of conditions at the antitriptic level. The validity and potential for practical application of the antitriptic flow approximation can be tested by comparing the moisture flux convergence computed via (19) to that computed using the actual surface wind field.

7. Case studies

Approximately 30 cases have been run for a variety of severe weather situations. Since the evaluation is subjective, it is not clear how to compare the fields in a statistical fashion. Thus, we have chosen some representative cases, with the primary emphasis on a "typical" case, for presentation. This case occurred on 13 June 1976, the day that a violent tornado occurred at Jordan, Iowa. Some details of this case have been presented by Brown and Knupp (1980). Iowa tornado locations shown in Fig. 6 have been adapted from their paper. Based on satellite imagery, the storm which produced this

series of tornadoes first developed about 1300 CST at the location shown by an x in Fig. 7. The tornadoes formed shortly before 1400 CST and dissipated about 1530 CST.

Initial storm development did not take place in the surface moisture maxima, but rather in an area characterized by strong cross-isobaric flow and a large horizontal pressure gradient at 1200 CST (Fig. 7). By 1500 CST, the two small low-pressure centers consolidated into a single, deeper, "subsynoptic" low (Fig. 8) with the severe weather concentrated in the northeast quadrant of the low, as described by Doswell (1977).

At 1200 CST there is a marked difference between the surface and the antitriptic moisture flux convergence fields. The surface field (Fig. 9a) has two convergence maxima, each one associated with a surface mixing ratio maximum. On the other hand, the antitriptic moisture flux convergence (Fig. 9b) is characterized by a single maximum, which intrudes toward the severe weather zone. While the conventional moisture flux convergence maximum in Kansas and southeastern Nebraska argues the importance of the dryline, the antitriptic field correctly indicates that the more important feature is the trough line connecting the two small lows.

By 1500 CST the conventional (Fig. 10a) and the antitriptic (Fig. 10b) moisture flux convergence fields have come into closer agreement. Again, the antitriptic field correctly indicates strong thunderstorms in east central Iowa, outside of the region of significant conventional moisture convergence. Further, severe convection developed during the afternoon in northern Illinois, which is depicted as moisture divergent by the conventional analysis.

Although the improvement in this case is not dramatic, it is typical of how the antitriptic assumption tunes the moisture flux convergence field. Note that the antitriptic moisture flux convergence is contoured at twice the interval used for the conventional version, as a result of the higher antitriptic wind speeds.

In the examples to follow, the relative merits of the antitriptic versus the surface moisture flux convergence field vary. In some, the antitriptic computation depicts events more favorably than the 13 June 1976 case; in others, less so. No comparison of results is really valid without a more detailed examination of the four-dimensional atmospheric structure, but these secondary cases are suggestive of the potential value in the antitriptic flow concept.

Case number one (Fig. 11a) shows a fairly marked improvement by the antitriptic moisture flux convergence, over the conventional pattern. The cluster of storm reports in north-central Oklahoma is much closer to the antitriptic maximum, even though the whole area is convergent in the conventional analysis.
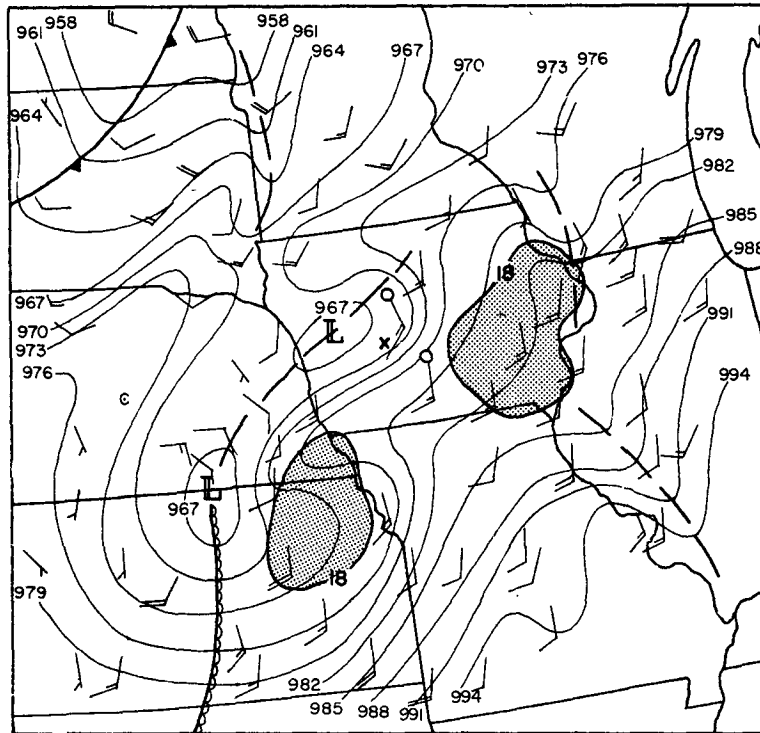
FIG. 7. Surface analysis of altimeter setting at 1200 CST 13 June 1976 (isobars in hundreths of inches of Hg with leading digit suppressed). Stippling denotes surface mixing ratios in excess of 18 g kg^{-1}. Dryline is denoted by scalloped line. Fort Dodge and Des Moines, Iowa are located by the open station circles.
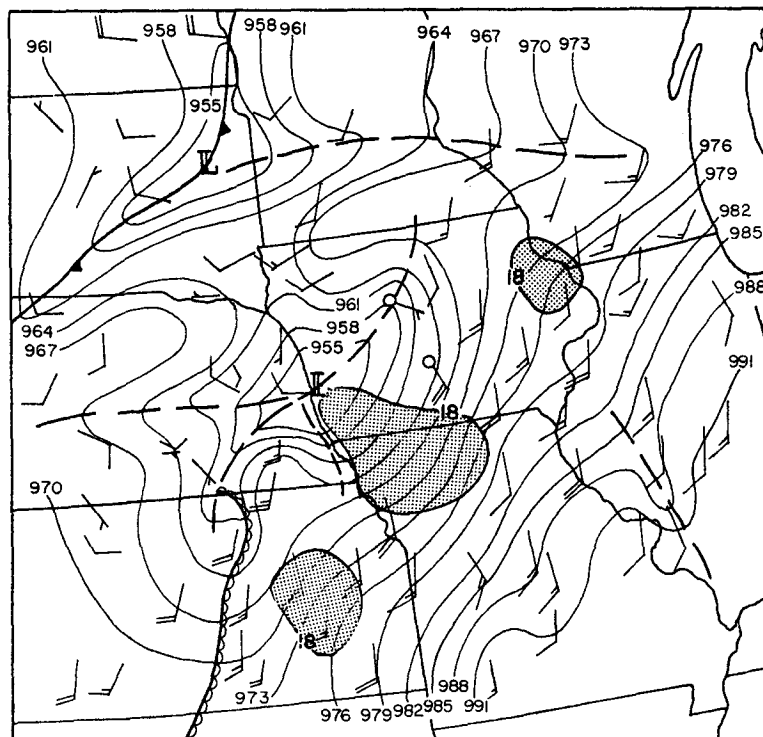
FIG. 8. Surface analysis at 1500 CST 13 June 1976.
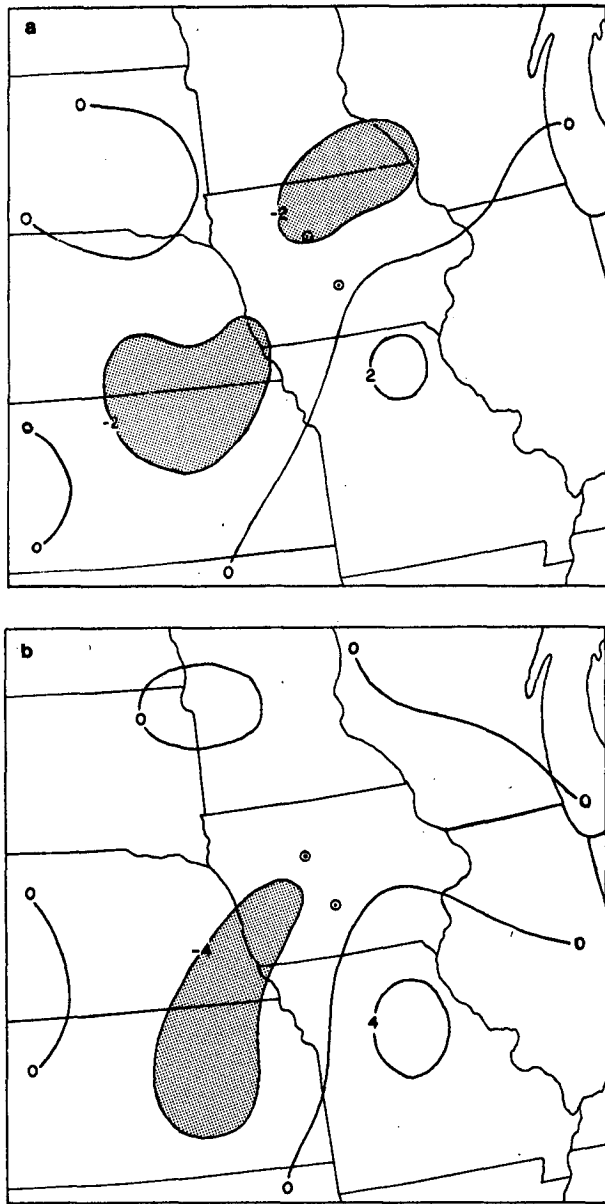Contours and symbols as in Fig. 7.

FIG. 9. Moisture flux divergence at 1200 CST 13 June, 1976 $(10^{-4}$ g kg^{-1} s$^{-1})$. Fort Dodge and Des Moines, Iowa are located by the circled dots. (a) Computed with surface data; (b) computed with antitriptic wind.

Case number two (Fig. 11b—the day following case one) is somewhat ambiguous. Although both methods have captured the main cluster of severe weather in northeastern Texas, the antitriptic flow suggests a second center in Arkansas much more strongly. However, the reports in extreme eastern Arkansas and northwestern Mississippi are between centers in the antitriptic field. Reports in western Tennessee are caught by the antitriptic flow field and missed by the conventional. It would seem, for this case, that a merger of the two fields would be most appropriate.

Case number three (Fig. 11c) is similarly ambiguous. The severe reports in eastern Iowa and northwestern Illinois are on the margins of the antitriptic moisture flux convergence, while the death-dealing tornado in northeast Kansas is well-handled.

Case number four (Fig. 11d), a relatively modest outbreak of severe thunderstorms, shows that the antitriptic threat area captures more of the reports, but includes a fairly large region where no severe weather occurred.

8. Summary

Since geostrophic equilibrium is inherently inappropriate for a surface-layer approximation to the
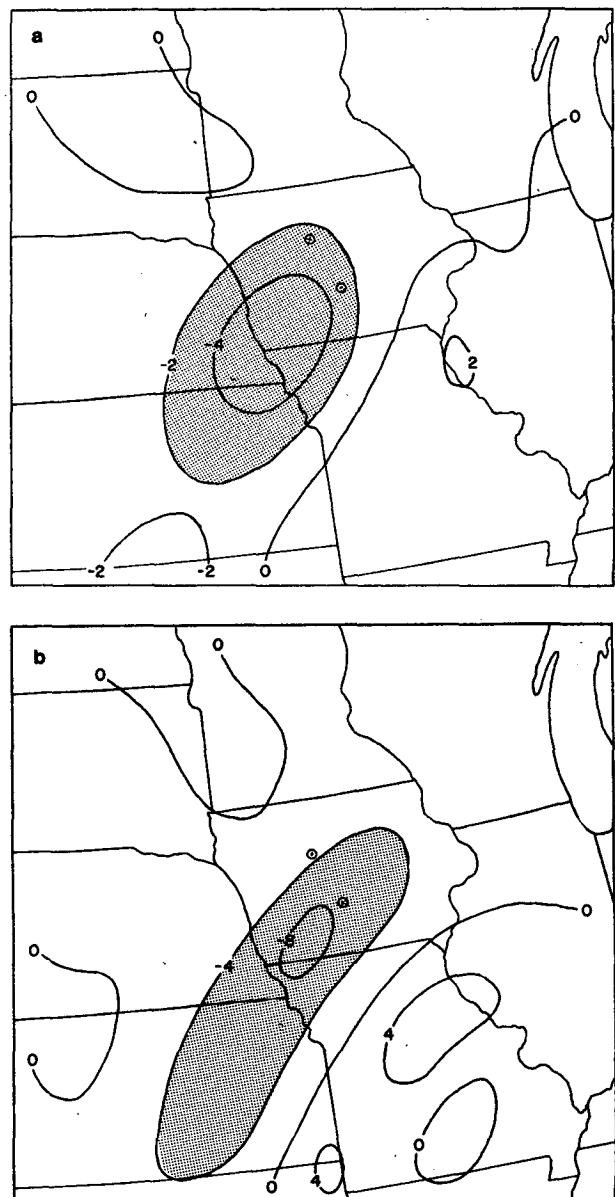

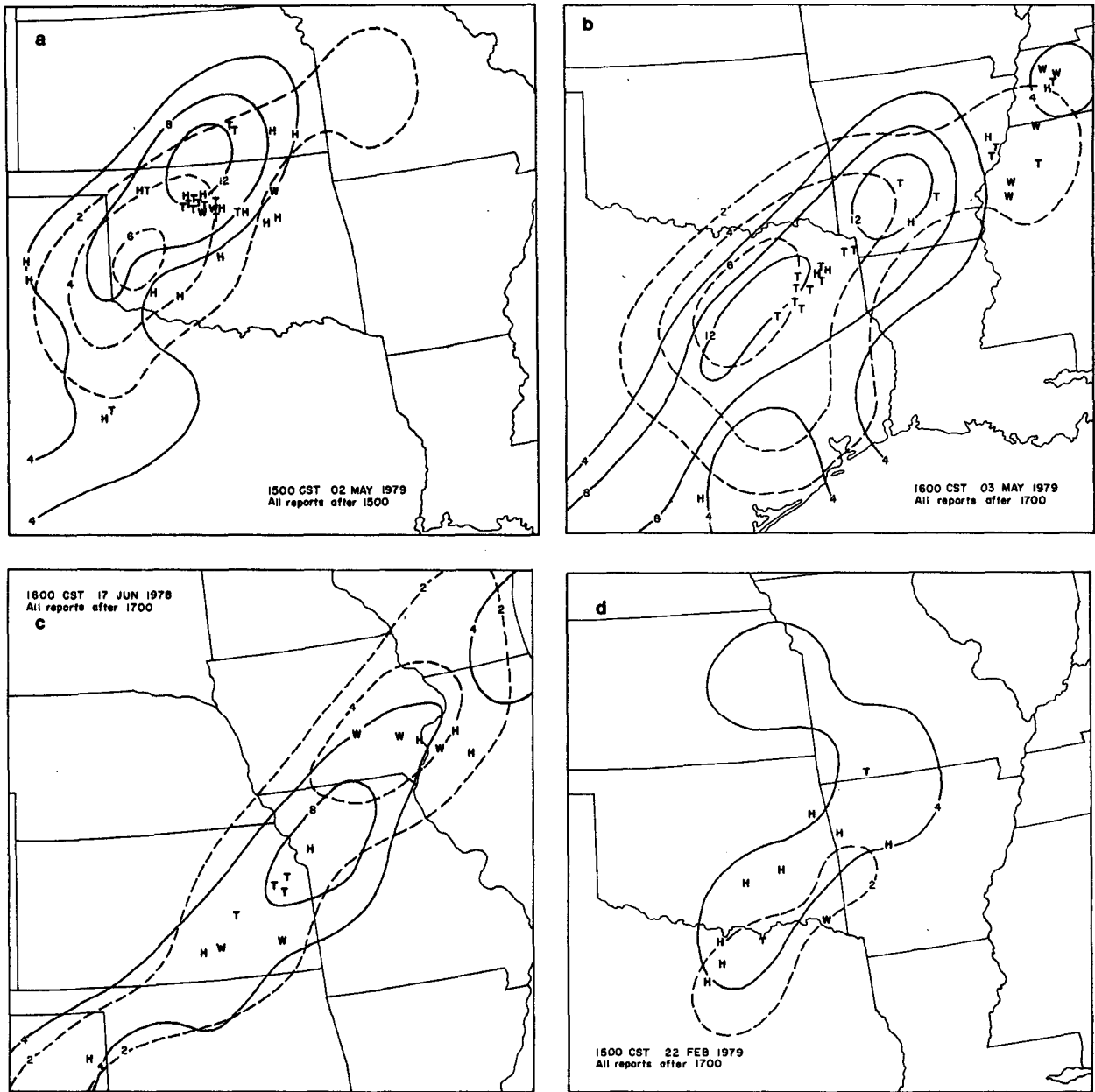FIG. 10. As in Fig. 9 except at 1500 CST 13 June 1976.

FIG. 11. Surface moisture flux convergence (dashed), antitriptic moisture flux convergence (solid) in 10^{-4} g kg^{-1} s^{-1}, and severe weather reported after map time until midnight (T tornado, H hail $\geq$ ¾ inch, W wind gust $\geq$ 50 kt or reported wind damage). (a) 1500 CST 2 May 1979; (b) 1600 CST 3 May 1979; (c) 1600 CST 17 June 1978; (d) 1500 CST 22 February 1979.

steady-state flow, some estimate of frictional forces is required for the maximum utilization of surface observations. The relatively crude approximation of frictional stresses via a Guldburg-Mohn coefficient elucidates several features of the low-level flow.

By making some reasonable assumptions, the behavior of the flow as it approaches a state of antitriptic balance from an initially unbalanced state can be solved analytically. It is seen that the real wind is driven toward the antitriptic wind with an e-folding time of several hours. Further, the

divergence and vorticity both undergo a damped oscillation during adjustments. However, the divergence transient has larger amplitude and can be as much as 90° out of phase with the vorticity transient. The results show that the vorticity approaches its antitriptic value nearly monotonically, while the divergence transient can significantly overshoot its equilibrium state before most of the adjustment is completed. One phenomenon which exhibits several features of this theory is the low-level jet of the Great Plains. The nocturnal shift of the vertical velocity

field from left to right across the low-level jet axis can, to some extent, be explained by the antitriptic adjustment of divergence.

As a test of the antitriptic balance concept's *practical* validity, a comparison is made between moisture flux divergence calculated directly from observed surface data and that obtained using antitriptic winds. The basic question examined is whether or not antitriptic flow, derived solely from surface data, is a better estimate of severe storm inflow than the observed surface winds. The case studies suggest that antitriptically computed moisture flux divergence is at least as good as, and generally somewhat better than, that computed using surface wind vectors. Therefore, the indication is that the simple concept of antitriptic balance can be of value for inferring processes immediately above the contact layer.

REFERENCES

Arya, S. P. S., 1978: Comparative effects of stability, baroclinity and the scale-height ratio on drag laws for the atmospheric boundary layer. *J. Atmos. Sci.*, **35**, 40–46.

Bonner, W. D., 1966: Case study of thunderstorm activity in relation to the low-level jet. *Mon. Wea. Rev.*, **94**, 167–178.

——, S. Esbensen and R. Greenberg, 1968: Kinematics of the low-level jet. *J. Appl. Meteor.*, **7**, 339–347.

——, and J. Paegle, 1970: Diurnal variations in boundary layer winds over the south-central United States in summer. *Mon. Wea. Rev.*, **98**, 735–744.

Brown, J. M., and K. R. Knupp, 1980: The Iowa cyclonic-anticyclonic tornado pair and its parent thunderstorm. Submitted to *Mon. Wea. Rev.*

Ching, J. K. S., and J. A. Businger, 1968: The response of the planetary boundary layer to time varying pressure gradient force. *J. Atmos. Sci.*, **25**, 1021–1025.

Cressman, G. P., 1960: Improved terrain effects in barotropic forecasts. *Mon. Wea. Rev.*, **88**, 327–342.

Day, S., 1953: Horizontal convergence and the occurrence of summer precipitation at Miami, Florida. *Mon. Wea. Rev.*, **81**, 155–161.

Defant, F., 1951: Local Winds. *Compendium of Meteorology*, T. F. Malone, Ed., Amer. Meteor. Soc., 655–672.

Doswell, C. A. III, 1976: Subsynoptic-scale dynamics as revealed by use of filtered surface data. NOAA Tech. Memo. ERLTM-NSSL-79, 40 pp. [NTIS PB 265-433/AS].

——, 1977: Obtaining meteorologically significant surface divergence fields through the filtering property of objective analysis. *Mon. Wea. Rev.*, **105**, 885–892.

Guldburg, G. M., and H. Mohn, 1876: *Études sur les Mouvements de l'Atmosphère*. I. A. W. Brögger, Oslo.

Hudson, H. R., 1971: On the relationship between horizontal moisture convergence and convective cloud formation. *J. Appl. Meteor.*, **10**, 755–762.

Huschke, R. E., 1959: *Glossary of Meteorology*. Amer. Meteor. Soc., 638 pp.

Lewis, J. M., 1971: Variational subsynoptic analysis with applications to severe local storms. *Mon. Wea. Rev.*, **99**, 786–795.

Mahrt, L., 1975: The influence of momentum advections on a well-mixed layer. *Quart. J. Roy. Meteor. Soc.*, **101**, 1–11.

——, and S. U. Park, 1976: The influence of boundary layer pumping on synoptic-scale flow. *J. Atmos. Sci.*, **33**, 1505–1520.

Mellor, G. L., and T. Yamada, 1974: A hierarchy of turbulence closure models for planetary boundary layers. *J. Atmos. Sci.*, **31**, 1791–1806.

Negri, A. J., D. W. Hillger and T. H. Von der Haar, 1977: Moisture convergence from a combined mesoscale moisture analysis. *Preprints 10th Conf. Severe Local Storms*, Omaha, Amer. Meteor. Soc., 48–53.

Ogura, Y., and Y-L Chen, 1977: A life history of an intense mesoscale convective storm in Oklahoma. *J. Atmos. Sci.*, **34**, 1458–1476.

Paegle, J., and J. Paegle, 1978: Frictional effects in strongly divergent flows. *J. Atmos. Sci.*, **35**, 1197–1203.

Saucier, W. J., 1955: *Principles of Meteorological Analysis*. The University of Chicago Press, 438 pp.

Schaefer, J. T., 1976: Moisture features of the convective boundary layer in Oklahoma. *Quart. J. Roy Meteor. Soc.*, **102**, 447–451.

——, and C. A. Doswell III, 1979: On the interpolation of a vector field. *Mon. Wea. Rev.*, **107**, 458–476.

Starr, J. G., 1945: Note on inertial oscillations. *J. Meteor.*, **2**, 120–122.

Tennekes, H., and J. L. Lumley, 1972: *A First Course in Turbulence*. The MIT Press, 300 pp.

Ulanski, S. L., and M. Garstang, 1978: The role of surface divergence and vorticity in the life cycle of convective rainfall. Part I: Observations and analysis. *J. Atmos. Sci.*, **35**, 1047–1062.

Wilkins, E. M., and Y. Sasaki, 1970: Drag coefficient for a hurricane. *Summary, Conf. on Wind Loads on Structures*, Cal Tech, Pasadena, National Science Foundation [Available from authors on request.]